JACS
JOURNAL OF THE AMERICAN CHEMICAL SOCIETY

Article

pubs.acs.org/JACS

Rectangular Bunched Rutile TiO_2 Nanorod Arrays Grown on Carbon Fiber for Dye-Sensitized Solar Cells

Wenxi Guo,[†,‡] Chen Xu,[†] Xue Wang,[†] Sihong Wang,[†] Caofeng Pan,[†] Changjian Lin,*[,‡] and Zhong Lin Wang*[,†]

[†]School of Material Science and Engineering, Georgia Institute of Technology, Atlanta, Georgia 30332, United States

[‡]State Key Laboratory of Physical Chemistry of Solid Surfaces, College of Chemistry and Chemical Engineering, Xiamen University, Xiamen 361005, China

Supporting Information

ABSTRACT: Because of their special application in photovoltaics, the growth of one-dimensional single-crystalline TiO_2 nanostructures on a flexible substrate is receiving intensive attention. Here we present a study of rectangular bunched TiO_2 nanorod (NR) arrays grown on carbon fibers (CFs) from titanium by a "dissolve and grow" method. After a corrosion process in a strong acid solution, every single nanorod is etched into a number of small nanowires. Tube-shaped dye-sensitized solar cells are fabricated by using etched TiO_2 NR-coated CFs as the photoanode. An absolute energy conversion efficiency of 1.28% has been demonstrated under 100 mW cm^{-2} AM 1.5 illumination. This work demonstrates an innovative method for growing bunched TiO_2 NRs on flexible substrates that can be applied in flexible devices for energy harvesting and storage.

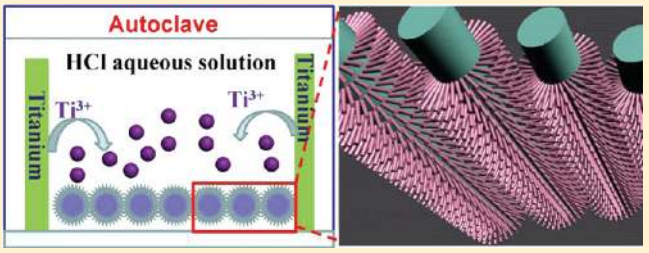

INTRODUCTION

The insufficient fossil-fuel-based energy supplies and excessive CO_2 emissions are the two major issues for the current global energy strategies. Searching for "green" energy resources is one of the most urgent challenges for the sustainable development of human civilization, which could be potentially solved by renewable energy technology.[1−8] As one of the most promising photovoltaic technologies, dye-sensitized solar cells (DSSCs) have received intensive attention.[9−12] A conversion efficiency of more than 11% has been obtained by adopting a photoanode that consists of a TiO_2 nanocrystal thin film covered by a monolayer of dye molecules.[13,14] However, this kind of cell is usually based on a rigid fluorine-doped tin oxide (FTO) glass subtrate that is not suitable for transportation, installation, and remote application. To strengthen the adaptability of DSSCs, polymer substrates,[15,16] metal sheets,[17] or metal wires[18,19] have been used as substrates to fabricate DSSCs. At the same time, in practical applications, polymer substrates are limited by their poor thermostability, while metallic substrates are not very stable in the electrolyte that contains iodine (I^{3+}/I^{+}). To solve this problem, a substrate that could be widely used is highly desirable for this technology.

Here we introduce a fiber-shaped solar cell based on carbon fibers (CFs). Relative to the traditional photoanode, CFs are flexible, conductive, and stable in liquid electrolyte, and they can supply a large surface area, which is critical for nanostructure-based photovoltaic technology. They also have good heat resistance and fatigue. Moreover, CFs could be a promising candidate to be built into weavelike solar cells that can be fabricated into clothes. Although this material shows the possibility of application for DSSCs, a method for effective growth of commonly used anode materials on the CFs for DSSCs is still an issue,[20−22] especially for single-crystal TiO_2 nanorods (NRs) or nanowires (NWs). To date, most of the TiO_2 nanostructures on CFs have been limited to amorphous TiO_2 nanoparticles obtained by sol−gel methods.[23,24] However, the TiO_2 nanoparticles obtained by sol−gel methods are not crystalline, and high temperature with protected gas is required for calcination to form the crystalline phase. Moreover, the material quality is not very good because of the uneven surface and the existence of cracks when increasing the thickness. An ideal solution for preparing TiO_2 nanostructures or films on CFs is direct growth of orderly one-dimensional and single-crystalline TiO_2 NWs on the CFs. A direct connection of TiO_2 NWs with the substrate may improve the DSSC performance. Specifically, oriented single-crystalline TiO_2 NRs or NWs on a conductive substrate without annealing would be most desirable,[25,26] but achieving these structures has been limited by the availability of synthetic techniques. Herein we introduce a new method that includes "dissolve and grow" and "etch and grow" processes to prepare ultrafine and uniform, single-crystal TiO_2 NWs on CFs.

Received: December 25, 2011

   dx.doi.org/10.1021/ja2120585 | J. Am. Chem. Soc. XXXX, XXX, XXX−XXX

EXPERIMENTAL SECTION

A schematic illustration of the growth of NRs on the CFs is shown in Figure 1A. In a typical synthesis process, 0.025−0.1 g of Ti foil and 18 mL of 0.05−0.1 M HCl solution were put into a Teflon-lined stainless steel autoclave with a total volume of 25 mL. The CFs were then immersed into the solution after ultrasonic cleaning for 30 min in a 1:1:1 (v/v/v) mixture of acetone, ethanol, and deionized water. The hydrothermal synthesis was conducted at 423−463 K for 2−18 h in an electric oven. The autoclave was cooled to room temperature with flowing water for 10 min after the growth process. Next, the CFs were ultrasonically cleaned for 3 min in a 2:1 (v/v) mixture of isopropanol and water. The thus-cleaned CFs with TiO_2 NRs around them were transferred into Teflon-lined stainless steel autoclave again and treated in the 9−27% HCl solution at 433−463 K for 2−10 h for the etching process. The resulting CFs with TiO_2 NRs around them were immersed in 100 mL of 0.2 M $TiCl_4$ aqueous solution for 6−8 h and then annealed in argon at 723 K for 30 min to increase crystallinity.

The resulting CFs with TiO_2 NRs around them were sensitized in a 0.3 mM solution of *cis*-bis(isothiocyanato)bis(2,2′-bipyridyl-4, 4′-dicarboxylato)ruthenium(II) bis(tetrabutylammonium) dye (N-719 as received from Solaronix) in dry ethanol for 24 h. Tube-shaped solar cells were assembled according to the method introduced by Zou and co-workers:[27] first, the N719-sensitized CFs were wound uniformly and spirally onto a platinum-coated optical fiber, which was then inserted into the sealing capillary (Φ = 0.5 mm). The internal space of the device was filled with a liquid electrolyte [0.5 M LiI, 50 mM I_2, and 0.5 M 4-*tert*-butylpyridine in 3-methoxypropionitrile (Fluka)] by the capillary effect.

The morphology and microstructure of the TiO_2 nanostuctures were examined by scanning electron microscopy (SEM) using a LEO 1530 scanning electron microscope and by transmission electron microscopy (TEM) using Hitachi HF2000 and JEOL 4000EX transmission electron microscopes. Phase identification of TiO_2 was conducted by X-ray diffraction (XRD) using a PANalytical X'Pert PRO diffractometer. A SoLux solar simulator was used as calibrated with a Daystar meter to simulate sunlight for an illumination intensity of 100 mW cm^{-2}. The solar cell was irradiated using a solar simulator (500 W model 91160, Newport) with an AM 1.5 spectrum distribution calibrated against an NREL reference cell to simulate accurately a full-sun intensity (100 mW cm^{-2}). The irradiated length of this kind of tube-shaped three-dimensional (3D) DSSC from the side of the working electrode was 1−3 cm.

RESULTS AND DISCUSSION

Figure 1 shows typical SEM and TEM images of TiO_2 NRs grown on the CFs after hydrothermal reaction at 463 K for 3 h. As can be seen from Figure 1B,C, the entire surfaces of the CFs are covered very uniformly by TiO_2 NRs that are tetragonal in shape with square top facets. A cross-sectional view of the TiO_2 NRs is shown in Figure 1D; the diameter and length of the NRs were found to be ∼150 nm and ∼3 μm, respectively. The phase and crystal structure of the TiO_2 NRs were confirmed by the lattice image of Figure 1E. The distances between lattice fringes, 0.32 and 0.29 nm, can be assigned to (110) and (001) of the rutile TiO_2 phase, respectively, suggesting that the TiO_2 NRs grew along the [001] axis. The corresponding selected-area electron diffraction (SAED) pattern (Figure 1F) displays the single-crystalline nature and could be indexed to the pure rutile TiO_2 phase. The XRD pattern of the CFs covered by TiO_2 NRs is shown in Figure S1A in the Supporting Information (SI). All of the reflection peaks can be readily indexed to pure rutile TiO_2.

Figure 1A shows the schematic diagram of the formation mechanism of TiO_2 NRs by the "dissolve and grow" method, and it may be described by the following chemical reactions:[28]

$$2Ti + 6HCl \rightarrow 2TiCl_3 + 3H_2(g)$$

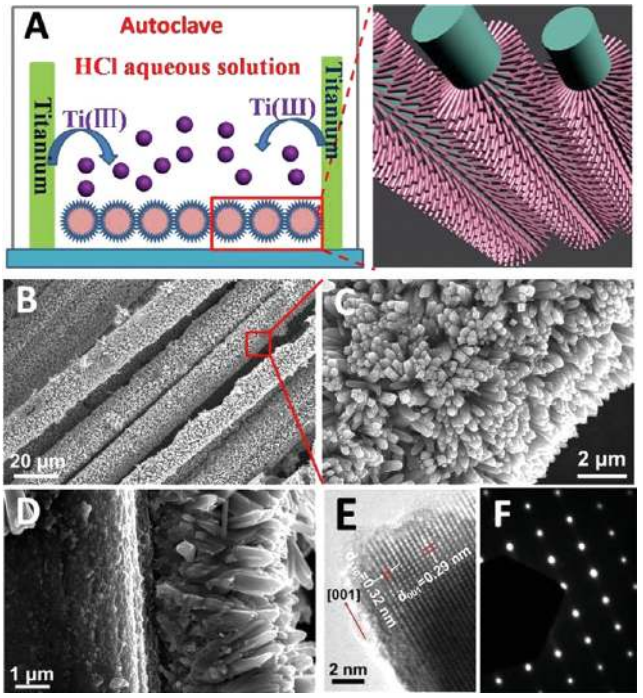

Figure 1. (A) Schematic representation of the growth of TiO_2 nanorod (NR) arrays on carbon fibers (CFs) by the "dissolve and grow" method. (B, C) SEM images of the top view of TiO_2 NR arrays on CFs. (D) Cross-sectional view of the well-aligned TiO_2 NR arrays. (E) HRTEM image of a single TiO_2 NR. (F) SAED pattern of the same TiO_2 NR.

$$Ti^{3+} + H_2O \rightarrow TiOH^{2+} + H^+$$

$$TiOH^{2+} + O_2 \rightarrow Ti(IV)\text{−oxo species} + O_2 \rightarrow TiO_2$$

At the very beginning, in the presence of HCl, Ti foil reacts with H^+ at high temperature and pressure and gradually dissolves, continually releasing the Ti(III) precursors into the reaction solution. Because Ti(III) is not stable in aqueous solution, $TiOH^{2+}$ is produced by hydrolysis of Ti(III). According to the suggestion by Fujihara and co-workers,[28] $TiOH^{2+}$ is oxidized to Ti(IV) by reaction with dissolved oxygen. The Ti(IV) complex ions are thus used as the growth units, and the formation mechanism of the rutile TiO_2 NRs may be described as follows: For rutile TiO_2, a TiO_6 octahedron forms first by bonding of a Ti atom and six oxygen atoms. The TiO_6 octahedron then shares a pair of opposite edges with the next octahedron, forming a chainlike structure. Because the growth rate of the different crystal faces depends on the numbers of corners and edges of the coordination polyhedra available, the growth of rutile NRs follows the sequence (110) < (100) < (101) < (001).[29,30] Thus, rutile TiO_2 NRs growing along the [001] direction are formed.

According to the XRD pattern shown in Figure S1B in the SI, the CFs have an amorphous structure. Apparently, there is no lattice match between rutile TiO_2 and the CF substrate. Therefore, it is impossible for TiO_2 NRs to grow on the fiber surface through epitaxial growth. To provide a better understanding of the growth mechanism of this process, controlled experiments were carried out on a CF substrate by varying the acid concentration. In the reaction process, the acid not only acts as a reactant to dissolve Ti but also plays an important role

dx.doi.org/10.1021/ja2120585 | J. Am. Chem. Soc. XXXX, XXX, XXX−XXX

in restricting the hydrolysis rate of Ti(III) by providing an acidic environment.

When the concentration of HCl is low, the Ti foil dissolves relatively slowly, and the concentration of the Ti(IV) precursor is also very low at the beginning. However, when most of the Ti is dissolved, the growth rate of TiO_2 nanorods becomes much faster than before as a result of not only the increased concentration of the Ti(IV) precursor but also the consumption of HCl, which obviously increases the pH of the solution. More and more Ti(III) produced in the solution leads to a high degree of supersaturation of Ti(IV), and thus, a large number of polycrystalline clusters form in the solution by homogeneous nucleation. Next, these clusters are deposited on the surface of the CF and act as the nucleating centers for further growth of nanorods. Because there is no crystal plane trend for these clusters, nanorods can grow along any direction and then self-assemble into microspheres or tufted nanoflowers, as shown in Figure 2A,B. The microsphere/microflower film

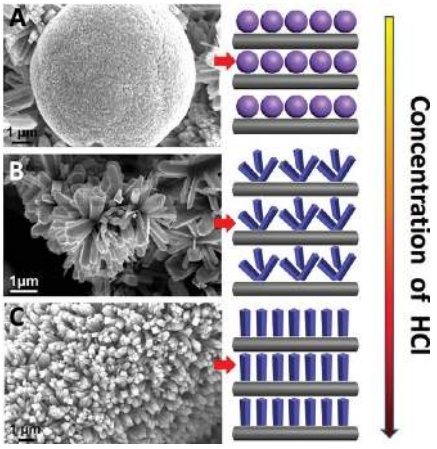

Figure 2. SEM images of the TiO_2 nanostructures obtained at different concentrations of HCl on CFs: (A) 0.5 M; (B) 1 M; (C) 1.67 M. The corresponding schematic diagrams represent the growth processes of TiO_2 nanostructures on CFs.

does not firmly adhere to the CF substrate and can easily be peeled off.

When the concentration of HCl is moderate, the reaction proceeds more smoothly because of the "double buffer" effect of HCl. For the "double buffer" effect, first, HCl strictly controls the dissolution rate of Ti, which guarantees that the concentration of Ti(III) is not too high or too low. Second, the consumption of HCl does not obviously decrease the concentration of H^+ when the concentration of HCl is moderate, so a stable acidic environment is maintained, effectly restricting the hydrolysis of Ti(IV). Therefore, the hydrothemal solution maintains a low degree of supersaturation. Because of the "double buffer" effect of HCl, it is difficult for TiO_2 polycrystalline clusters to form in the solution by homogeneous nucleation; instead, the low degree of supersaturation favors heterogeneous nucleation on the surface of CFs. Figure S2 in the SI shows the SEM images of a rutile TiO_2 NR film grown on the CF substrate at 463 K for different times. When the hydrothermal treatment time was 1 h, we can observe that lots of very tiny TiO_2 nucleations form on the CF surface; some formed TiO_2 nanorods are also shown in Figure S2B. When the hydrothermal treatment time is increased, the growth of NRs is very fast, and the substrate is completely covered by NRs after 2.5 h of hydrothermal treatment (Figure S2D). Microspheres and microflowers do not form under these conditions.

When the concentration of HCl is high, nothing is grown on the CFs, and the solution is clear even after reaction for over 16 h at 463 K. This may be due to the fact that the high acidity seriously restricts the hydrolysis of Ti(III) and restrains both homogeneous and heterogeneous nucleations.

The diameters of the obtained TiO_2 nanorods on CFs are 150−500 nm, which are too large for applications in many fields. To increase the surface area of the TiO_2 NRs further, we treated them in hydrochloric acid solution at 453 K for 3−5 h. The obtained NRs were characterized by SEM and TEM, as shown in Figure 3. It can be obviously seen that a different

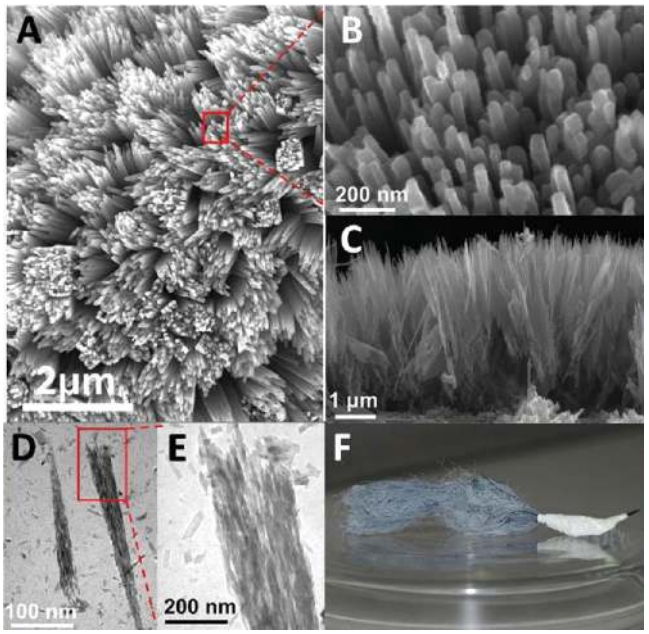

Figure 3. (A, B) Top-view SEM images of bunched TiO_2 NR arrays after hydrothermal treatment in HCl solution at 453 K for 4 h at (A) low and (B) high magnification. (C) SEM cross-sectional view of the bunched TiO_2 NR arrays. (D, E) TEM images of the the corresponding bunched TiO_2 nanorod. (F) Optical photo of the carbon fibers coated by bunched TiO_2 nanorod arrays.

morphology was obtained after 4 h of hydrothermal treatment at 453 K. The top-view SEM images of the TiO_2 NRs in Figure 3A,B show that every single NR is etched into many smaller TiO_2 NWs ranging from 10 to 30 nm in diameter and oriented perpendicular to the (001) facet, while all of the the original NRs keep the rectangular outline. The cross-sectional view of the etched TiO_2 NRs in Figure 3C shows obvious etching traces on the top of the NRs. From the TEM images of the etched TiO_2 NRs in Figure 3D,E, it can be observed that a single NR is etched into many smaller NWs, which reveals that the NR can be etched from top to bottom before the formation of the nanotube. We call this kind of structure "rectangular bunched TiO_2 NRs". The formation mechanism of the orientation-aligned NRs can be explained as follows.

First of all, from the SEM image shown in Figure 4A, we can observe that the obtained TiO_2 NRs are aggregates of much smaller TiO_2 square crystals. Upon treatment with HCl solution, the etching rate in the grain boundaries of the crystals is much faster than in other places because of the greater number of defects and higher reactivity in the grain boundary.

dx.doi.org/10.1021/ja2120585 | J. Am. Chem. Soc. XXXX, XXX, XXX−XXX

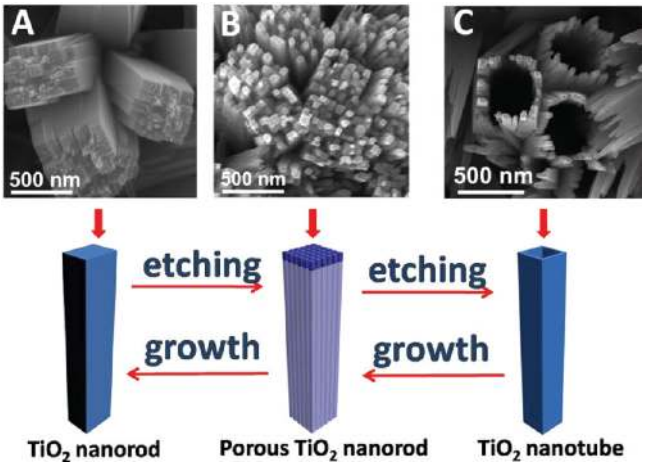

Figure 4. Formation mechanism of the rectangular bunched TiO_2 NR arrays and NT arrays. SEM images of (A) TiO_2 NR arrays, (B) bunched TiO_2 NR arrays, and (C) TiO_2 NT arrays are shown, and the corresponding schematic diagrams represent the growth mechanism of TiO_2 nanostructures on CFs.

With the continuous corrosion on the crystal boundaries, the densely packed TiO_2 square crystals are separated from each other, and the original TiO_2 NRs become many thinner NWs, as shown in Figures 3A and 4B. Moreover, these thin NWs are still not stable in the acidic solution, and when the hydrothermal treatment time is further increased, all of the NWs dissolve, producing rectangular nanotubes, as shown in Figure 4C and further confirmed by the TEM images in Figure S3 in the SI. According to the work of Liu et al.,[31] the formation mechanism of the TiO_2 nanotube (NT) arrays can be explained as follows.

When the NRs are treated with hydrochloric acid during the hydrothermal process, the HCl preferentially etches the TiO_2 NRs in the [001] direction because the (001) facet below is far more reactive than the crystalline facet of the side wall, causing the dissolution rate in the long-axis direction to be faster than that in the side-wall direction. This can explain why the formed NWs dissolve first and then leave the rectangular-shaped NTs. To provide further comfirmation of the mechanism for the formation of orientation-aligned NRs and NTs, we again used 0.025−0.1 g of Ti foil and 18 mL of 0.05−0.1 M HCl solution as growth solution, with the resulting rectangular TiO_2 NTs as the growth substrate. After different growth times, the bunched TiO_2 NRs and original TiO_2 NRs were obtained in succession again, revealing that the etching and growth process is reversible and providing further evidence that the more reactive crystalline facet is more reactive in both growth and corrosion.

It is worth mentioning that the TiO_2 NR film grown on the FTO substrate can easily be peeled off upon etching in the HCl solution. However, for the CF substrate, the film remains adhered to the CF surface and cannot be peeled off even when the outline of NTs begins to dissolve (Figure S4 in the SI). This may be attributed to the good bonding force and low surface tension between the CF surface and TiO_2 NRs.

To assemble the DSSCs, CFs covered with ~5 μm long TiO_2 NRs were used as photoanodes, and all of the photoanodes were treated with 0.2 M $TiCl_4$ for 6−8 h. The design and principle of the fiber-based solar cell is shown in Figure 5A. An optical fiber coated with platinum was used as the counter electrode. When sunlight irradiates the photoanode, which is sensitized with N719, the excited electrons are rapidly injected

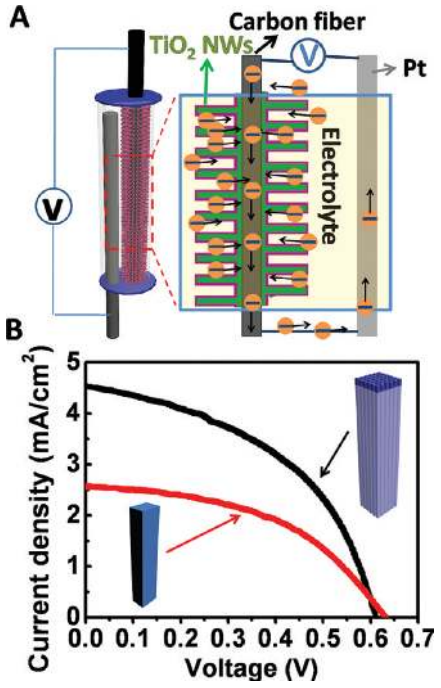

Figure 5. (A) Schematic representation of the configuration of the CF/TiO_2 NR array-based tube-shaped 3D DSSC. (B) J−V curves of DSSCs based on TiO_2 NR arrays and bunched TiO_2 NR arrays on CFs.

into the conduction band of the rutile TiO_2 NRs and transported along the CFs, from which they flow to the counter electrode through the external circuit. Current density−voltage (J−V) curves of these kinds of tube-shaped solar cells based on TiO_2 NRs and bunched NRs are shown in Figure 5B. Under 100 mW cm^{-2} AM 1.5 illumination, different performances were observed. For the NR-based solar cell, the short-circuit current density, open-circuit voltage, fill factor, and efficiency were J_{sc} = 2.57 mA/cm^2, V_{oc} = 0.63 V, FF = 0.47, and η = 0.76%, respectively, while for the bunched-NR-based solar cell, J_{sc} = 4.58 mA/cm^2, V_{oc} = 0.61 V, FF = 0.46, and η = 1.28%. The current density of the bunched-NR-based solar cell is larger than that in original NR-based solar cell, which can be attributed to the larger surface area of the bunched NRs, which enables more dye molecules to be adsorbed. The relatively low V_{oc} in both cells may be explained by the electron recombination at the interface of the CFs and the loss of light upon passage through the electrolyte.

The CF-based 3D DSSC has several outstanding features. First, from a configuration perspective, this tube-shaped solar cell can capture light from all directions, thus showing the potential of this system for applications under intensively focused sunlight.[27] Second, because of their high electrical conductivity, corrosion resistance toward I_2, high reactivity for triiodide reduction, and low cost, carbonaceous materials are quite attractive as possible replacements for platinum as counter electrodes,[32−34] and therefore, we can introduce CF or other carbon materials as the counter electrodes for this configuration. In this case, we can fabricate DSSCs based on carbon materials and TiO_2 that are promising as low-cost solar cells in the future. Third, CF-based solar cells are suitable to be fabricated into large-area solar cells by growth of the TiO_2 NRs on carbon paper or carbon cloth, which is very promising for integration into clothes in the future. Finally, the success in

dx.doi.org/10.1021/ja2120585 | J. Am. Chem. Soc. XXXX, XXX, XXX−XXX

growing ultrafine TiO_2 NWs on CFs is significant for their application in organic solar cells, photocatalysis, and lithium ion batteries.

In summary, we have developed an innovative and cost-effective approach for growing bunched TiO_2 NRs on CFs for enhancing the performance of DSSCs. The first step involves direct transformation of pure Ti into vertically aligned single-crystal TiO_2 NRs on the CFs using the "dissolve and grow" method. The second is to etch the TiO_2 NRs into bunched TiO_2 NRs using the hydrothermal method in strong acid condition. On the basis of the bunched TiO_2 NR-covered CFs, tube-shaped 3D DSSCs were assembled found to exhibit an efficiency of 1.28%, which is 68% higher than that of the original NRs. Combining the advantages of TiO_2 NRs and CFs, the hybrid structure can be applied in many fields, such as photocatalysis, gas sensing, organic solar cells, and lithium ion batteries. Furthermore, the growth of single-crystal TiO_2 nanostructures on conductive flexible substrates without high-temperature anealing may be beneficial for application in some flexible devices.

■ ASSOCIATED CONTENT

Supporting Information

XRD patterns of CFs with and without TiO_2 NRs on them, SEM images of TiO_2 NWs grown on CFs for different times, and TEM and SEM images of TiO_2 nanotubes grown on CFs. This material is available free of charge via the Internet at http://pubs.acs.org.

■ AUTHOR INFORMATION

Corresponding Author

cjlin@xmu.edu.cn; zlwang@gatech.edu

Notes

The authors declare no competing financial interest.

■ ACKNOWLEDGMENTS

The authors thank NSF and BES DOE for support. W.G. thanks the Chinese Scholars Council for support, and C.L. gratefully acknowledges the financial support from the National Natural Science Foundation of China (51072170, 21021002).

■ REFERENCES

(1) Tian, B.; Zheng, X.; Kempa, T. J.; Fang, Y.; Yu, N.; Yu, G.; Huang, J.; Lieber, C. M. *Nature* **2007**, *449*, 885.
(2) Wang, X. D.; Song, J. H.; Liu, J.; Wang, Z. L. *Science* **2007**, *316*, 102.
(3) Wang, Z. L. *Sci. Am.* **2008**, *298*, 82.
(4) Wang, Z. L.; Song, J. H. *Science* **2006**, *312*, 242.
(5) Dresselhaus, M. S.; Thomas, I. L. *Nature* **2001**, *414*, 332.
(6) Pan, C. F.; Fang, Y.; Wu, H.; Ahmad, M.; Luo, Z. X.; Li, Q. A.; Xie, J. B.; Yan, X. X.; Wu, L. H.; Wang, Z. L.; Zhu, J. *Adv. Mater.* **2010**, *22*, 5388.
(7) Gur, I.; Fromer, N. A.; Geier, M. L.; Alivisatos, A. P. *Science* **2005**, *310*, 462.
(8) Bisquert, J.; Cahen, D.; Hodes, G.; Ruhle, S.; Zaban, A. *J. Phys. Chem. B* **2004**, *108*, 8106.
(9) Oregan, B.; Grätzel, M. *Nature* **1991**, *353*, 737.
(10) Bach, U.; Lupo, D.; Comte, P.; Moser, J. E.; Weissortel, F.; Salbeck, J.; Spreitzer, H.; Grätzel, M. *Nature* **1998**, *395*, 583.
(11) Lee, K.; Park, S. W.; Ko, M. J.; Kim, K.; Park, N. G. *Nat. Mater.* **2009**, *8*, 665.
(12) Varghese, O. K.; Paulose, M.; Grimes, C. A. *Nat. Nanotechnol.* **2009**, *4*, 592.
(13) Grätzel, M. *J. Photochem. Photobiol., A* **2004**, *168*, 235.
(14) Grätzel, M. *Acc. Chem. Res.* **2009**, *42*, 1788.
(15) Durr, M.; Schmid, A.; Obermaier, M.; Rosselli, S.; Yasuda, A.; Nelles, G. *Nat. Mater.* **2005**, *4*, 607.
(16) Lindstrom, H.; Holmberg, A.; Magnusson, E.; Lindquist, S. E.; Malmqvist, L.; Hagfeldt, A. *Nano Lett.* **2001**, *1*, 97.
(17) Kang, M. G.; Park, N. G.; Ryu, K. S.; Chang, S. H.; Kim, K. J. *Sol. Energy Mater. Sol. Cells* **2006**, *90*, 574.
(18) Fan, X.; Chu, Z. Z.; Wang, F. Z.; Zhang, C.; Chen, L.; Tang, Y. W.; Zou, D. C. *Adv. Mater.* **2008**, *20*, 592.
(19) Liu, Z. Y.; Misra, M. *ACS Nano* **2010**, *4*, 2196.
(20) Zou, D. C.; Wang, D.; Chu, Z. Z.; Lv, Z. B.; Fan, X. *Coord. Chem. Rev.* **2010**, *254*, 1169.
(21) Li, Z. T.; Wang, Z. L. *Adv. Mater.* **2011**, *23*, 84.
(22) Unalan, H. E.; Wei, D.; Suzuki, K.; Dalal, S.; Hiralal, P.; Matsumoto, H.; Imaizumi, S.; Minagawa, M.; Tanioka, A.; Flewitt, A. J.; Milne, W. I.; Amaratunga, G. A. J. *Appl. Phys. Lett.* **2008**, *93*, 133116.
(23) Yuan, R. S.; Guan, R. B.; Shen, W. Z.; Zheng, J. T. *J. Colloid Interface Sci.* **2005**, *282*, 87.
(24) Yuan, R. S.; Zheng, J. T.; Guan, R. B.; Zhao, Y. C. *Colloids Surf., A* **2005**, *254*, 131.
(25) Liu, B.; Aydil, E. S. *J. Am. Chem. Soc.* **2009**, *131*, 3985.
(26) Feng, X. J.; Shankar, K.; Varghese, O. K.; Paulose, M.; Latempa, T. J.; Grimes, C. A. *Nano Lett.* **2008**, *8*, 3781.
(27) Fu, Y. P.; Lv, Z. B.; Hou, S. C.; Wu, H. W.; Wang, D.; Zhang, C.; Chu, Z. Z.; Cai, X.; Fan, X.; Wang, Z. L.; Zou, D. C. *Energy Environ. Sci.* **2011**, *4*, 3379.
(28) Hosono, E.; Fujihara, S.; Kakiuchi, K.; Imai, H. *J. Am. Chem. Soc.* **2004**, *126*, 7790.
(29) Cheng, H. M.; Ma, J. M.; Zhao, Z. G.; Qi, L. M. *Chem. Mater.* **1995**, *7*, 663.
(30) Kumar, A.; Madaria, A. R.; Zhou, C. W. *J. Phys. Chem. C* **2010**, *114*, 7787.
(31) Liu, L.; Qian, J. S.; Li, B.; Cui, Y. M.; Zhou, X. F.; Guo, X. F.; Ding, W. P. *Chem. Commun.* **2010**, *46*, 2402.
(32) Kay, A.; Grätzel, M. *Sol. Energy Mater. Sol. Cells* **1996**, *44*, 99.
(33) Roy-Mayhew, J. D.; Bozym, D. J.; Punckt, C.; Aksay, I. A. *ACS Nano* **2010**, *4*, 6203.
(34) Hou, S. C.; Cai, X.; Fu, Y. P.; Lv, Z. B.; Wang, D.; Wu, H. W.; Zhang, C.; Chu, Z. Z.; Zou, D. C. *J. Mater. Chem.* **2011**, *21*, 13776.